JOURNAL OF PROPULSION AND POWER
Vol. 27, No. 2, March–April 2011

Nonlinear Weighted-Least-Squares Estimation Approach for Gas-Turbine Diagnostic Applications

Y. G. Li*
Cranfield University, Cranfield, England MK43 0AL, United Kingdom
and
T. Korakianitis†
Queen Mary University of London, London, England E1 4NS, United Kingdom

DOI: 10.2514/1.47129

Gas-turbine engines are subject to degradation, or even failure, during their operation. Effective diagnosis of engine health would provide maintenance engineers with important engine health information, which can be used to achieve high engine availability and low maintenance costs. In this paper a novel gas-turbine health estimation technique is introduced, which is called nonlinear weighted-least-squares estimation. The nonlinear weighted-least-squares diagnostic method is an improvement to the conventional linear weighted-least-squares diagnostic method. It aims to provide an effective alternative to gas-turbine gas-path diagnostic analysis for condition monitoring. In the nonlinear weighted-least-squares estimation method the gas-turbine health parameters are estimated by minimizing the summation of weighted square deviations between estimated and actual values of gas-turbine performance measurements. The measurement uncertainties associated with gas-path measurements are taken into account by using a weighting matrix. The concepts of fault cases and gas-path-analysis index are introduced. These provide a new diagnostic approach, enabling fault isolation and enhancing the confidence of diagnostic results. This diagnostic approach allows the typically nonlinear gas-turbine thermodynamic-performance models to be directly used in condition monitoring while taking into account performance nonlinearities. An iterative calculation process is introduced to obtain a converged estimation of engine degradation. The nonlinear weighted-least-squares diagnostic approach has been applied to a model industrial gas-turbine engine to test its effectiveness. The numerical tests of the new diagnostic approach show that with appropriate selection of engine gas-path measurements, the method can be used effectively and successfully to predict gas-turbine performance degradation.

Nomenclature

CN_1	=	relative shaft rotational speed of the gas generator
DH	=	enthalpy drop
FC	=	flow capacity, kg/s
$h()$	=	thermodynamic function describing gas-turbine performance
J	=	weighted squares deviation
K	=	total number of component fault cases
K_s	=	total number of the most likely component fault cases
l	=	number of measurable parameters
m	=	number of ambient and operating condition parameters
m_f	=	fuel flow rate, kg/s
N	=	shaft relative rotational speed
n	=	number of engine health parameters
P	=	total pressure, atm
PR	=	pressure ratio
R	=	weighting matrix for measurable parameters
SF	=	degradation index or scaling factor
T	=	total temperature, K
$\mathbf{v}$	=	measurement noise vector
W	=	engine power output, MW
$\mathbf{w}$	=	ambient and operating condition parameter vector
$\mathbf{x}$	=	engine health parameter vector
$\mathbf{z}$	=	gas-path measurement vector
Γ	=	flow capacity
γ	=	gas-path analysis index
Δ	=	deviation
ε	=	relative estimation error
η	=	isentropic efficiency
λ	=	element of R
σ	=	convergence threshold
ω	=	underrelaxation factor

Subscripts

amb	=	ambient condition
c	=	compressor
deg	=	degradation
Eff	=	isentropic efficiency
t	=	turbine
1	=	engine inlet
3	=	compressor exit
8	=	compressor-driving-turbine (gasifier turbine) outlet
10	=	power turbine outlet

Received 10 September 2009; revision received 15 October 2010; accepted for publication 15 November 2010.

*Lecturer of School of Engineering; i.y.li@cranfield.ac.uk.
†Professor and Chair of Energy Engineering; korakianitis@alum.mit.edu.

I. Introduction

GAS turbine engines are subject to performance degradation due to fouling, corrosion, erosion, blade tip clearance damage, foreign and domestic object damage, etc. Many gas-turbine performance-based diagnostic methods for the detection of engine degradation have been developed since the first gas-path analysis (GPA) method was introduced in early 1970s [1]. Different gas-path diagnostic methods have been developed since then and examples of them are GPA and its derivatives [1–9], neural networks [10–12], Bayesian belief networks [13], genetic algorithms [14–16], fuzzy logic [17–19], diagnostics using transient measurements [20,21], etc. Recent comprehensive reviews on these technologies are provided in [22–24]. The linear weighted-least-squares estimation method for gas-turbine diagnostics [25] is one of the GPA derivatives and has been successfully used in industry. It is based on linear engine performance models and takes into account the estimation uncertainties

for engine health parameters and measurement uncertainties for gas-path measurements. Chen and Zhu [25] developed a model-identification-based fault analysis method to take into account the nonlinearity of engine performance in a weighted-least-squares method. Although linear GPA approaches have been successfully used in the past due to their simplicity (they use linear gas-turbine performance models), significant prediction errors may appear because of the actual nonlinear performance behavior of gas-turbine engines with degradation effects. This performance degradation results in component efficiency reductions. Component efficiencies must be concurrently optimized in order to maximize gas-turbine performance, and small changes in the efficiency of one component have significant effects on cycle performance and cycle optimization [26–31]. Different nonlinear-model-based gas-path diagnostic approaches have been proposed that take into account the nonlinearity of gas-turbine performance in gas-path diagnostic analysis in order to improve diagnostic accuracy. Typical examples of them are Newton–Raphson iterative application of linear GPA [7], conventional optimization-based approaches [32,33], and genetic-algorithm-based approaches [14,34].

In this paper, a novel nonlinear weighted-least-squares (NLWLS) estimation method is introduced and is applied to gas-turbine gas-path diagnostic applications. The NLWLS method is combined with the fault-case concept [34] and the GPA index [8], to form a new gas-path diagnostic approach for effective gas-turbine fault detection, isolation and quantification. The accuracy and confidence of the diagnostic results are assessed with the values of the GPA indices. This approach allows the use of nonlinear gas-turbine thermodynamic-performance models and takes into account the impact of gas-path measurement noise. An iterative solution process is introduced to obtain a converged solution. To test the effectiveness of the approach the NLWLS diagnostic method is applied to a model industrial gas-turbine engine similar to GE LM2500+.

II. Nonlinear Weighted-Least-Squares Diagnostic Approach

The performance of a gas-turbine engine behaves nonlinearly in different ambient, operating, and engine health conditions. The functional relationship between the engine health parameters $\mathbf{x}$, ambient and operating condition parameters $\mathbf{w}$, and measurable parameters $\mathbf{z}$ can be expressed by

$$\mathbf{z} = h(\mathbf{x}, \mathbf{w}) + \mathbf{v} \tag{1}$$

where $\mathbf{z} \in R^l$ is a dependent parameter vector or engine gas-path measurable parameter vector; l is the number of the parameters (examples of such parameters are gas-path temperatures, pressures, shaft rotational speeds, fuel flow rate, thrust, shaft power, etc.); $\mathbf{x} \in R^n$ is an independent or engine health parameter vector, where n is the number of the parameters; $\mathbf{w} \in R^m$ is an ambient and operating condition parameter vector, where m is the number of the parameters; $h()$ is a thermodynamic function describing gas-turbine engine performance behavior; and $\mathbf{v} \in R^l$ is a measurement noise vector corresponding to $\mathbf{z}$.

The vector $\mathbf{x}$ refers to engine health parameters of major engine components such as compressors and turbines. The degradation of a compressor may be described by the deviation of three degradation indices relevant to its isentropic efficiency, flow capacity, and pressure ratio. A typical compressor characteristic map is shown in Fig. 1, where the relationship among four compressor characteristic parameters (i.e., pressure ratio PR_c, isentropic efficiency η_c, flow capacity FC_c, and relative rotational speed CN_c) at different operating conditions is represented. The solid lines represent the clean (i.e., not-degraded) compressor map, and the dotted lines represent the degraded compressor map. A compressor may (more or less) keep its original geometry although small damage to the compressor may occur as the result of compressor degradation, such as fouling, erosion, corrosion, tip clearance wearing, etc. The change of the compressor characteristic map can be represented by a relative shift of speed lines. Such shift may occur in three parameters: PR_c, FC_c, and η_c respectively. The quantity of the shift is represented by three compressor health parameters: pressure ratio index $\mathrm{SF}_{c,\mathrm{PR}}$, flow-capacity index $\mathrm{SF}_{c,\mathrm{FC}}$, and efficiency index $\mathrm{SF}_{c,\mathrm{Eff}}$, defined by Eqs. (2–4). These equations represent the ratios between the values of corresponding points on degraded speed lines (dotted lines in Fig. 1) and original speed lines (solid lines in Fig. 1):

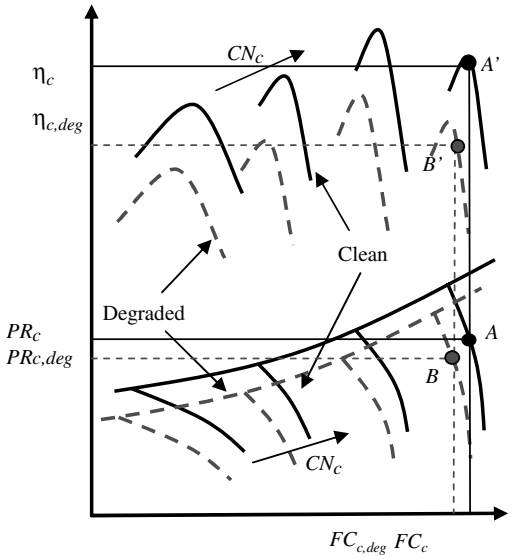

Fig. 1 Clean and degraded compressor characteristics map.

$$\mathrm{SF}_{c,\mathrm{FC}} = \mathrm{FC}_{c,\mathrm{deg}}/\mathrm{FC}_c \tag{2}$$

$$\mathrm{SF}_{c,\mathrm{PR}} = \mathrm{PR}_{c,\mathrm{deg}}/\mathrm{PR}_c \tag{3}$$

$$\mathrm{SF}_{c,\mathrm{Eff}} = \eta_{c,\mathrm{deg}}/\eta_c \tag{4}$$

These three degradation indices are independent from each other. The variations of $\mathrm{SF}_{c,\mathrm{FC}}$ and $\mathrm{SF}_{c,\mathrm{PR}}$ have a similar effect on the shift of a compressor map, and for simplicity they are assumed to be equal, so that

$$\mathrm{SF}_{c,\mathrm{FC}} = \mathrm{SF}_{c,\mathrm{PR}} \tag{5}$$

The turbine degradation is represented in a manner similar to compressor degradation, by the deviation of three degradation indices relevant to its isentropic efficiency, flow capacity, and enthalpy drop. A typical turbine characteristic map is shown in Fig. 2. The relationship among four turbine characteristic parameters is represented (namely, flow capacity, enthalpy drop, isentropic efficiency, and relative rotational speed) at different operating conditions. The solid lines represent the clean (not-degraded) turbine characteristics, and the dotted lines represent degraded characteristics. Three degradation indices may be used to describe the shift of the characteristic map due to turbine degradation, and they are flow-capacity index $\mathrm{SF}_{t,\mathrm{FC}}$, enthalpy drop index $\mathrm{SF}_{t,DH}$, and isentropic efficiency index $\mathrm{SF}_{t,\mathrm{Eff}}$, given by Eqs. (6–8):

$$\mathrm{SF}_{t,\mathrm{FC}} = \mathrm{FC}_{t,\mathrm{deg}}/\mathrm{FC}_t \tag{6}$$

$$\mathrm{SF}_{t,DH} = DH_{t,\mathrm{deg}}/DH_t \tag{7}$$

$$\mathrm{SF}_{t,\mathrm{Eff}} = \eta_{t,\mathrm{deg}}/\eta_t \tag{8}$$

These three degradation indices are independent from each other. The increase of $\mathrm{SF}_{t,\mathrm{FC}}$ has a similar effect on the shift of a turbine map to that of the decrease of $\mathrm{SF}_{t,DH}$; thus, for simplicity it is assumed that

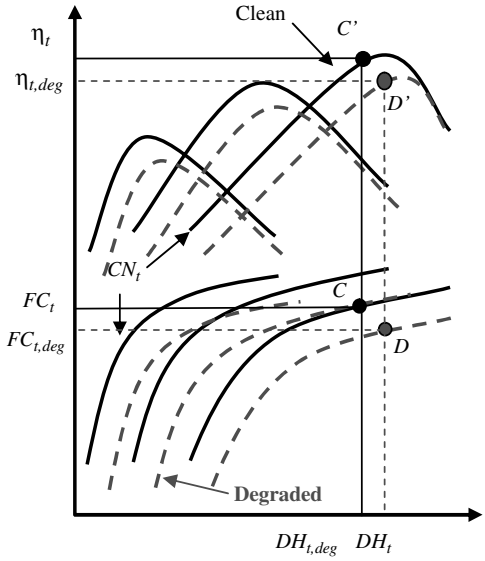

Fig. 2 Clean and degraded turbine characteristics map.

$$\mathrm{SF}_{t,\mathrm{FC}} = \frac{1}{\mathrm{SF}_{t,DH}} \tag{9}$$

When an engine operates at an unchanged nominal ambient and operating condition (specified for engine diagnostic analysis purposes) Eq. (1) can be expressed by

$$\mathbf{z} = h(\mathbf{x}) + \mathbf{v} \tag{10}$$

$$\begin{bmatrix} z_1 \\ z_2 \\ \vdots \\ z_l \end{bmatrix} = \begin{bmatrix} h_1(\underline{x}) \\ h_2(\underline{x}) \\ \vdots \\ h_l(\underline{x}) \end{bmatrix} + \begin{bmatrix} v_1 \\ v_2 \\ \vdots \\ v_l \end{bmatrix} \tag{11}$$

The deviation of the health parameters and measurable parameters from their true values can be measured with weighted square deviations J, which are expressed by Eq. (12) or Eq. (13):

$$J = (\hat{\mathbf{x}} - \mathbf{x})^T(\hat{\mathbf{x}} - \mathbf{x}) + (\mathbf{z} - h(\mathbf{x}))^T R(\mathbf{z} - h(\mathbf{x})) \tag{12}$$

or

$$J = \sum_{i=1}^{n}(\hat{x}_i - x_i)^2 + \sum_{j=1}^{l}\lambda_j \cdot (z_j - h_j(\mathbf{x}))^2 \tag{13}$$

where $R \in R^{l\times l}$ is a weighting matrix for gas-path measurable parameters,

$$R = \begin{bmatrix} \lambda_1 & 0 & \dots & 0 \\ 0 & \lambda_2 & 0 & \dots \\ \dots & 0 & \ddots & 0 \\ 0 & \dots & 0 & \lambda_l \end{bmatrix} \tag{14}$$

and $\hat{\mathbf{x}}$ is the estimation of $\mathbf{x}$.

The absolute values of the parameters involved in Eq. (13) may differ significantly in quantity, and it is more convenient to use normalized difference values of the parameters; therefore, Eq. (13) becomes

$$\bar{J} = \sum_{i=1}^{n}\left(\frac{\hat{x}_i - x_i}{\hat{x}_i}\right)^2 + \sum_{j=1}^{l}\lambda_j \cdot \left(\frac{z_j - h_j(\mathbf{x})}{z_j}\right)^2 \tag{15}$$

$\bar{J}$ needs to be minimized to best estimate the engine health parameters $\mathbf{x}$. This minimization is expressed by

$$\partial\bar{J}/\partial\mathbf{x} = \mathbf{0} \tag{16}$$

or

$$\frac{\partial\bar{J}}{\partial\mathbf{x}} = \begin{bmatrix} \partial\bar{J}/\partial x_1 \\ \partial\bar{J}/\partial x_2 \\ \vdots \\ \partial\bar{J}/\partial x_n \end{bmatrix} = \mathbf{0} \tag{17}$$

The solution of Eq. (16) or Eq. (17) provides the minimum error in the weighted-least-squares sense. To solve Eq. (16) or Eq. (17), Eq. (17) can be expanded as

$$\frac{\partial\bar{J}}{\partial x_i} = -\left(\frac{\hat{x}_i - x_i}{\hat{x}_i}\right) - \sum_{j=1}^{l}\lambda_j \cdot \left(\frac{z_j - h(\mathbf{x})}{z_j}\right) \cdot \left(\frac{\partial(h_j(\mathbf{x})/z_j)}{\partial(x_i/\hat{x}_i)}\right) = 0$$
$$(i = 1, 2, \dots, n) \tag{18}$$

and therefore

$$x_i = \hat{x}_i + \hat{x}_i \cdot \sum_{j=1}^{l}\lambda_j \cdot \left(\frac{z_j - h_j(\mathbf{x})}{z_j}\right) \cdot \left(\frac{\partial(h_j(\mathbf{x})/z_j)}{\partial(x_i/\hat{x}_i)}\right)$$
$$(i = 1, 2, \dots, n) \tag{19}$$

An iterative calculation process is introduced to solve the set of multiple equations (19). The iterative solution is described as follows.

Suppose that $\hat{x}_{i,k}$ is a previous estimate of x_i. A new estimate $\hat{x}_{i,k+1}$ can be expressed with

$$\hat{x}_{i,k+1} = \hat{x}_{i,k} + \omega\cdot\hat{x}_{i,k}\cdot\sum_{j=1}^{l}\left\{\lambda_j\cdot\left(\frac{z_j - h_j(\hat{\mathbf{x}}_k)}{z_j}\right)\cdot\left(\frac{\partial(h_j(\hat{\mathbf{x}})/z_j)}{\partial(x_i/\hat{x}_i)}\bigg|_{\mathbf{x}=\mathbf{x}_k}\right)\right\}$$
$$(i = 1, 2, \dots, n) \tag{20}$$

where ω is an underrelaxation factor with a value between 0 and 1, to be chosen to improve the convergence.

The objective of gas-turbine health status estimation is to isolate degraded gas-turbine components and quantify the deviation of component health parameters of the degraded components.

All gas-turbine components may degrade during operation. However, some components may degrade much faster and much more severely than others. If such a priori information is available, only those most severely degraded components may be selected for health status estimation. A schematic illustration of an iterative process of the NLWLS approach for gas-turbine health status estimation targeting at the selected potential degraded components is shown in Fig. 3. At a certain ambient and operating conditions, and when the engine is degraded after a period of operation, an engine performance model is used to simulate the performance at the same condition with estimated degradation $\hat{\mathbf{x}}$. The engine component degradation $\mathbf{x}$ is estimated with Eq. (20) in an iterative process until the convergence criteria represented in Eq. (21) are satisfied:

$$\Delta = \sum_{j=1}^{l}\left\{\lambda_j \cdot \left(\frac{z_j - h_j(\hat{\mathbf{x}})}{z_j}\right) \cdot \left(\frac{\partial(h_j(\hat{\mathbf{x}})/z_j)}{\partial(x_i/\hat{x}_i)}\right)\right\} < \sigma \tag{21}$$

where σ is a very small number (0.001 is chosen in this study).

The estimation error for each gas-path measurement is represented by the relative difference between the predicted and actual measurable parameters and expressed with

$$\varepsilon_i = \frac{z_{i,\mathrm{predicted}} - z_{i,\mathrm{actual}}}{z_{i,\mathrm{actual}}} \times 100\% \tag{22}$$

where ε_i is the estimation error for the ith gas-path measurement parameter.

To assess the prediction accuracy and confidence of the diagnostic results, a GPA index γ [8] defined by Eq. (23) is used:

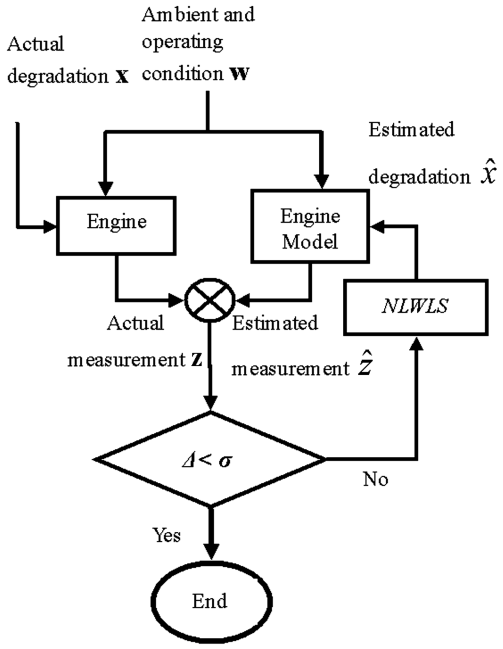

Fig. 3 Schematic illustration of iterative NLWLS approach.

$$\gamma = \frac{1}{1+\varepsilon} \tag{23}$$

where ε is a measure of the difference between the deviations of the actual and predicted engine measurable parameters expressed with Eq. (24):

$$\varepsilon = \frac{1}{l}\sum_{i=1}^{l} |\varepsilon_i| \tag{24}$$

where ε_i is defined in Eq. (22).

Because of the large number of potential engine health parameters when all the potential degraded engine components are included in a diagnostic analysis using the above iterative solution (Fig. 3), significant smearing effect may appear in the solution where the predicted component degradation may be distributed among both actually degraded and not-degraded components. This may provide users confusing degradation information and result in the actual degraded component(s) not being accurately identified. In addition, some components may degrade much more quickly and significantly than others, although all components may degrade simultaneously. It is therefore possible to catch the most severely degraded components by assuming a maximum number of severely degraded components in a diagnostic searching process. Therefore, the concept of engine fault cases introduced by Zedda and Singh [34] and Volponi et al. [35] (where each possible combination of potentially degraded components is regarded as a fault case) is used to isolate degraded components. Based on fault-case concept, a maximum number of simultaneously degraded engine components and the component fault cases (CFC) that cover all the possible combination of potentially degraded components should be considered. For example, compressor degradation can be one fault case and a combined compressor and power turbine degradation can be another. Then the diagnostic approach proposed in Fig. 3 is applied to each of the fault cases. If a preassumed fault case is chosen correctly, the predicted gas-path measurements will be very close to the actual measurements so the GPA index will be very close to 1 due to a very small value of ε. Therefore, a GPA index approaching the value 1 indicates a very accurate degradation prediction, and a GPA index close to 0 means the opposite. The highest value of the GPA indices obtained among all fault cases would indicate the most likely engine degradation cases. As a rule of thumb, when degraded components are correctly searched, the GPA indices will be above 0.85, and when not-degraded components are searched, the GPA indices will be below 0.75. Of course, such values may vary in different applications due to the impact of different levels of measurement accuracy and measurement noise. Even so, the difference in the GPA indices between the above two situations is a noticeable step change and such difference will be demonstrated in the test cases in a following section.

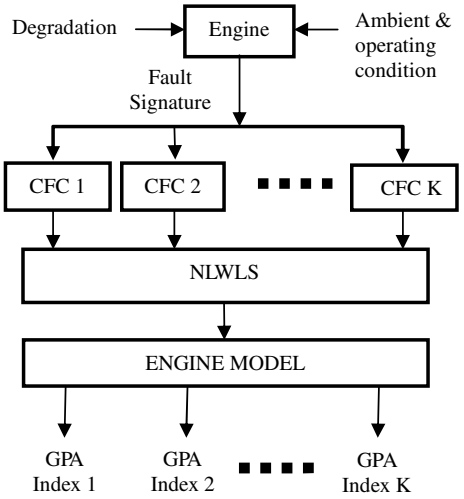

Fig. 4 NLWLS diagnostic approach using GPA index.

Figure 4 shows how the iterative NLWLS diagnostic approach can be applied to all potential fault cases (assuming total number of potential fault cases is K). At certain ambient and operating conditions, the engine fault signature expressed with the deviation of gas-path measurements from their baseline value is used as input information for performance degradation estimation. To isolate actual degraded engine components, the NLWLS approach will be used to search each of the potential fault cases and provide a solution for each fault case. Such predicted degradation for each fault case will then be input into the engine model to produce the predicted gas-path measurements and therefore calculate the corresponding GPA index.

In a situation in which more than one component fault case have high GPA indices, weighted degradation prediction is suggested and calculated as follows to obtain a unique solution:

$$\bar{\hat{x}}_i = \sum_{j=1}^{K_s} \hat{x}_{ij} \cdot \gamma_j \Big/ \sum_{j=1}^{K_s} \gamma_j \tag{25}$$

where $\bar{\hat{x}}_i$ is a weighted health parameter, $\hat{x}_{ij}$ is the ith health parameter predicted in component fault case j, γ_j is the GPA index in component fault case j, and K_s ($K_s < K$) is the total number of the most likely fault cases.

III. Application of NLWLS to Model Gas Turbine

The following is an example of applying the developed NLWLS approach to the diagnostic analysis of a model gas-turbine engine.

A. Model Gas-Turbine Engine

A representative model gas-turbine engine (Fig. 5) is chosen for the demonstration of how the NLWLS diagnostic approach is applied

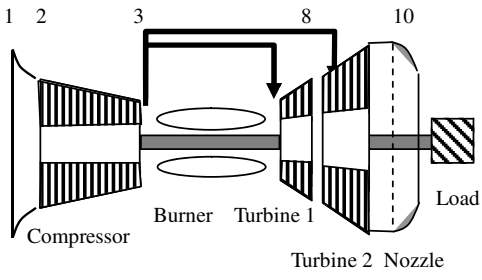

Fig. 5 Model gas-turbine configuration.

to gas-turbine gas-path diagnostic applications. It is a two-shaft industrial gas-turbine engine with one compressor, one burner, one compressor turbine, and one power turbine. It is assumed that the engine operates at standard International Organization for Standardization condition at sea level all the time, and the power output is kept constant by the engine control system, even when the engine is degraded. The basic performance specifications of the engine are as follows: total exhaust flow rate is 83 kg/s, total pressure ratio is 23.1, power output (dry) is 29 MW, and thermal efficiency is 38%.

A performance model for the model engine is created with Cranfield University gas-turbine performance and diagnostics software TURBOMATCH [36]/PYTHIA [8], whose validity has been proved over the years. Clean and degraded engine performance and gas-path measurements are simulated with TURBOMATCH/PYTHIA. A typical set of engine gas-path measurements like the set shown in Table 1 is selected to provide engine measurable information for gas-path diagnostic analysis. These measurements include ambient and operating condition parameters P_{amb}, T_{amb}, and W, which are maintained constant, and gas-path parameters such as P_3, T_3, P_8, T_8, P_{10}, T_{10}, CN_1, and m_f. It is assumed that there is no sensor fault during operation. To make the simulation more realistic, random measurement noise for all gas-path measurable parameters are included in the simulated measurement samples, where the maximum levels of measurement noise for different gas-path measurements take the values shown in Table 2 (from [37]). Figure 6 shows the simulated measurement samples of P_3, with a comparison with their true values when the model engine works at a degraded condition.

To test the NLWLS diagnostic approach, three engine degradation case studies are simulated, and the details of the degradation of the three case studies are shown in Table 3. In the first case study the compressor of the model engine is degraded. In the second case study the two turbines are degraded simultaneously. In the third case study

Table 1 Engine gas-path instrumentation set

No.	Symbols	Parameters
1	T_{amb}, K	Ambient temperature
2	P_{amb}, atm	Ambient pressure
3	W, MW	Power turbine power output
4	CN_1, %	Gas generator relative shaft speed
5	m_f, kg/s	Fuel flow rate
6	T_3, K	Compressor exit total temperature
7	P_3, atm	Compressor exit total pressure
8	T_8, K	Compressor turbine exit total temperature
9	P_8, atm	Compressor turbine exit total pressure
10	T_{10}, K	Power turbine exit total temperature
11	P_{10}, atm	Power turbine exit total pressure

Table 2 Maximum measurement noise (from [37])

Range	Typical error
	Pressure
3–45 psia	±0.5%
8–460 psia	±0.5% or 0.125 psia, whichever is greater
	Temperature
−65–290°C	±3.3°C
290–1000°C	$\pm\sqrt{2.5^2 + (0.0075 \cdot T)^2}$
1000–1300°C	$\pm\sqrt{3.5^2 + (0.0075 \cdot T)^2}$
	Fuel flow
Up to 250 kg/h	41.5 kg/h
Up to 450 kg/h	34.3 kg/h
Up to 900 kg/h	29.4 kg/h
Up to 1360 kg/h	23.7 kg/h
Up to 1815 kg/h	20.8 kg/h
Up to 2270 kg/h	23.0 kg/h
Up to 2725 kg/h	25.9 kg/h
Up to 3630 kg/h	36.2 kg/h
Up to 5450 kg/h	63.4 kg/h
Up to 12,260 kg/h	142.7 kg/h

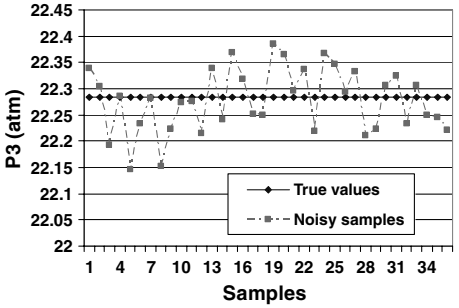

Fig. 6 Simulated measurement samples of P3.

different levels of degradation of the compressor are simulated sequentially (a sequential degradation of the compressor). The degradations are implanted into the model engine to simulate the corresponding gas-path measurements. A set of randomly selected measurement sample for each case study (with and without random measurement noise) is chosen. Figures 7 and 8 show the corresponding fault signatures, or the deviations of gas-path measurements, defined in Eq. (26) that are computed as the result of the simulated degradations:

$$\bar{z}_i = \frac{z_{i,\text{degraded}} - z_{i,\text{clean}}}{z_{i,\text{clean}}} \times 100\% \tag{26}$$

where $z_{i,\text{degraded}}$ is the ith measurement when the engine is degraded, and $z_{i,\text{clean}}$ is the same measurement when the engine is clean (not degraded). It can be seen that the fault signatures with measurement noise are slightly different to those without measurement noise. The measurement noise is random phenomena, and the single set of measurement noise conditions simulated on each of the measurement samples does not represent the whole image of the impact of measurement noise. A better analysis of the impact of measurement noise on diagnostic results can only be done by using a large number of measurement samples in order to obtain its statistical nature. However, it is not the intention of this study to investigate the statistic nature of the impact of measurement noise; the diagnostic analysis is limited to using individual measurement samples with the presence of measurement noise.

B. Diagnosis Using NLWLS in Three Case Studies

In the three case studies, it is assumed that the engine degradations (the implanted degradations) are unknown to the NLWLS diagnostics users, and only the fault signatures (Figs. 7 and 8) due to engine degradation are available. The following sample cases illustrate how the NLWLS approach is used to isolate and identify the degraded engine components.

It is assumed that the compressor and the two turbines of the model engine are the potentially degraded components. The number of simultaneously degraded components can be up to two, as discussed in Sec. II. Table 4 shows all the CFCs, i.e., all the possible combinations of engine component degradations, of the model engine.

1. *Results of Degradation Case Study 1*

Using the NLWLS diagnostic approach described in Fig. 4, all the possible fault cases (Table 4) are analyzed with the NLWLS approach using the fault signatures shown in Fig. 7. The corresponding GPA indices obtained from the diagnostic analysis are shown in Fig. 9.

Table 3 Degradation case studies

Case study	Degraded components	Implanted degradation, %
1	Compressor	$\Delta\eta_c = -1$, $\Delta\Gamma_c = -3$
2	Turbine 1	$\Delta\eta_t = -1$, $\Delta\Gamma_t = -3$
2	Turbine 2	$\Delta\eta_t = -1$, $\Delta\Gamma_t = -3$
3	Compressor	$\Delta\eta_c = 0.0$–2.0, $\Delta\Gamma_c = 0.0$–4.0

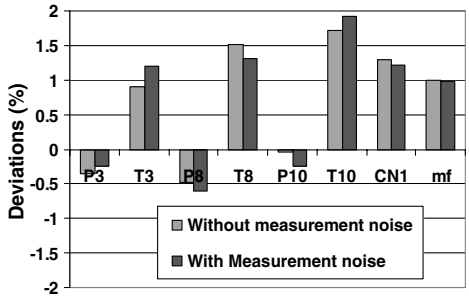

Fig. 7 Fault signatures due to implanted compressor degradation (degradation case study 1).

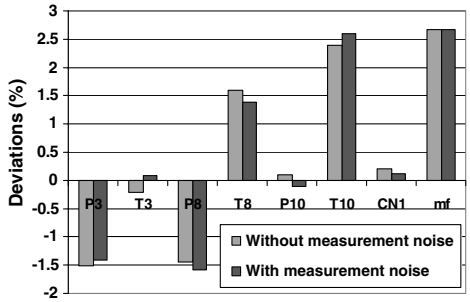

Fig. 8 Fault signatures due to implanted turbine 1 and 2 degradation (degradation case study 2).

Fault cases CFC1, CFC4, and CFC5 have the highest GPA indices: around 0.98 using fault signature without measurement noise and around 0.89 using fault signature with measurement noise. These indicate the most likely fault cases due to the higher values of the GPA indices. The measurement noise certainly has an effect on the prediction accuracy, but does not affect the most likely fault cases to be correctly identified. By looking at the three cases with high GPA indices in Fig. 9, it can be concluded that cases CFC1 (compressor only), CFC4 (compressor plus turbine 1), or CFC5 (compressor plus turbine 2) may indicate the degraded components. However, at the same time, the values for CFC2 (turbine 1 only) and CFC3 (turbine 2 only) are much lower, eliminating turbine 1 and turbine 2 as degraded components. The compressor is the common component that appears in all three fault cases. Therefore, it can be concluded that the compressor is the most likely degraded component in this case.

The predicted component degradations of the three most likely fault cases are compared and shown in Fig. 10 (where measurement noise is not included) and in Fig. 11 (where random measurement noise is included). Although the results of the predictions from the three most likely fault cases are similar, the solutions are slightly different. The smearing effect is noticeable in the turbines (Fig. 11).

To reduce the smearing effects and take the advantage of all the solutions from these three most likely fault cases, a weighted solution of the predicted engine degradation using Eq. (25) is obtained and shown in Fig. 12. This figure indicates that the compressor again has the largest degradation parameters, and the degradation parameters of the other components are so little that they can be neglected, strengthening the conclusion that only the compressor is the most likely degraded component. It also shows that the weighted solutions

Table 4 Engine component fault cases

Component fault case	Predefined faulty components
CFC1	Compressor
CFC2	Turbine 1
CFC3	Turbine 2
CFC4	Compressor and turbine 1
CFC5	Compressor and turbine 2
CFC6	Turbine 1 and turbine 2

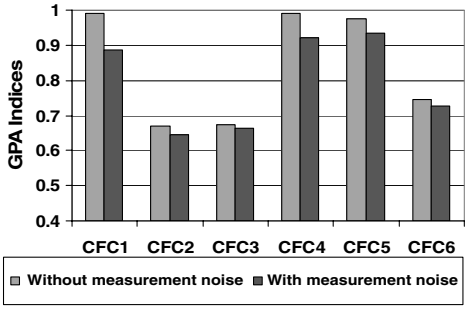

Fig. 9 GPA indices for all fault cases in case study 1.

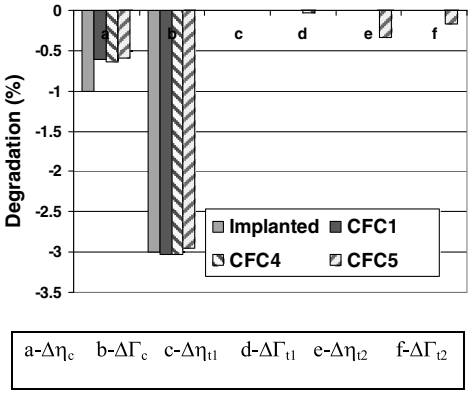

Fig. 10 Diagnostic results of most likely fault cases (without impact of measurement noise) in case study 1.

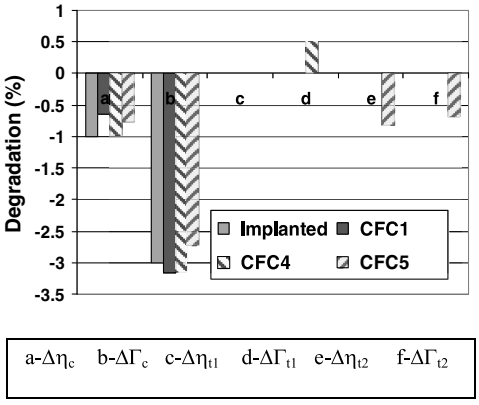

Fig. 11 Diagnostic results of most likely fault cases (with the impact of measurement noise) in case study 1.

are able to provide diagnostic results with smaller smearing effects and offer better predictions.

Based on the results in Figs. 9–12, the prediction errors for compressor flow-capacity indices is relatively smaller than those of the compressor efficiency indices. This may be due to the prediction accuracy of the NLWLS algorithm.

2. *Results of Degradation Case Study 2*

Similar to the case study 1, the NLWLS diagnostic approach described in Fig. 4 is applied to all the possible fault cases shown in Table 4 using the fault signature shown in Fig. 8 in case study 2. The corresponding GPA indices obtained from the diagnostic analysis are shown in Fig. 13. In this case, only fault case CFC6 has a much higher GPA index: around 0.98 using a fault signature without measurement noise and around 0.90 using a fault signature with random

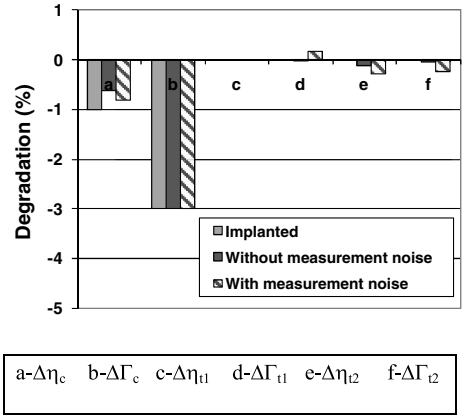

Fig. 12 Comparison of implanted and weighted diagnostic results in case study 1.

measurement noise. This indicates that the most likely fault case due to the higher value of GPA index is CFC6: the two turbines.

The predicted component degradations of the most likely fault case using fault signatures with and without measurement noise (Fig. 13) are compared with the implanted degradation and shown in Fig. 14. The predictions with both fault signatures (with and without random measurement noise) have very good prediction accuracy. The predictions with fault signatures without measurement noise have marginally better accuracy than those using fault signatures with measurement noise.

As there is only one fault case showing higher GPA index, the weighted solution using Eq. (25) is not necessary.

3. Results of Degradation Case Study 3

In this case study, nine sequential levels of gradually worsening compressor degradation were implanted into the model engine. The implanted degradation is shown with solid lines in Fig. 15, simulating a possible scenario in which the compressor degrades over time. The samples of the deviations of the gas-path measurements with the presence of random measurement noise

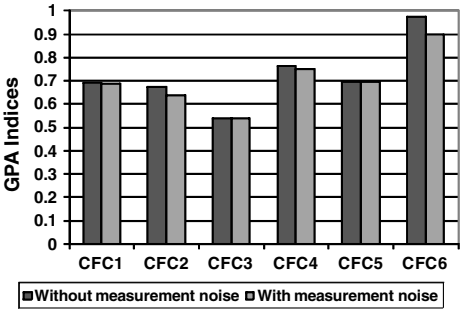

Fig. 13 GPA indices for all fault cases in case study 2.

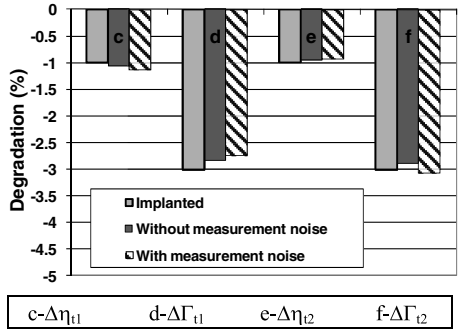

Fig. 14 Diagnostic results of the most likely fault case CFC6 (with and without impact of measurement noise) compared with implanted fault in case study 2.

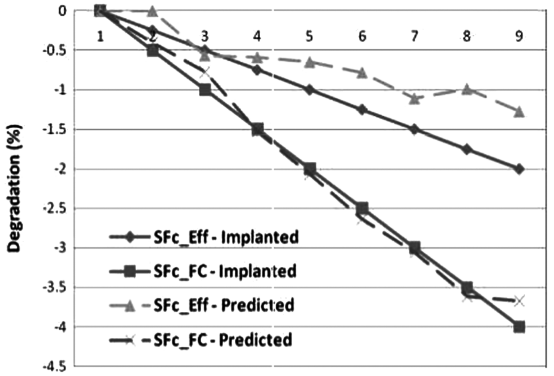

Fig. 15 Predicted degradation of case study 3.

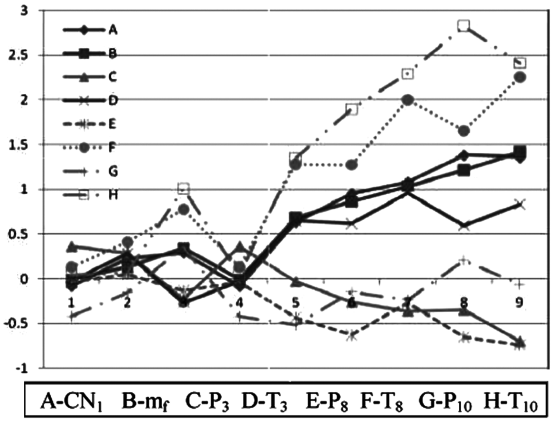

Fig. 16 Fault signatures of case study 3.

corresponding to the degraded conditions are simulated and shown in Fig. 16.

As the objective of this case study is to test how the developed NLWLS responds to different levels of degradation with the presence of measurement noise, only the compressor degradation is considered and analyzed in this typical example. The NLWLS is applied to the prediction of compressor degradation using the fault signatures at all nine points shown in Fig. 16. The predicted compressor degradations and their comparison with the implanted degradations are shown in Fig. 15. It can be seen that the predicted flow-capacity indices are very close to the actual ones, and the predicted efficiency indices are underestimated for most of the points, compared with the actual values. The inaccuracy of the predictions is similar to that in case study 1, caused by both the numerical algorithm and measurement noise. However, such level of accuracy should be acceptable for engineering applications. For all nine points, the GPA indices vary between 0.82 and 0.91 (Fig. 17). These are similar to the values of CFC1 in case study 1.

C. Discussion

The application of the NLWLS diagnostic approach to the model gas turbine shows promising results. This is indicated in Fig. 9 (case study 1) and Fig. 13 (case study 2), where the most likely degraded fault cases can be identified with the higher values of GPA indices, and in Fig. 12 (case study 1), Fig. 14 (case study 2), and Fig. 15 (case study 3), where the engine degradation can be quantified with good accuracy.

The measurement noise may have noticeable negative impact on the diagnostic prediction accuracy, such as the results shown in Fig. 11, where the smearing effect on the two turbines becomes noticeable, whereas the actual degradation occurs in the compressor. However, such impact does not affect the correct identification of the actual fault cases, particularly when the smearing effect is reduced by the application of the weighting of the most likely fault-case

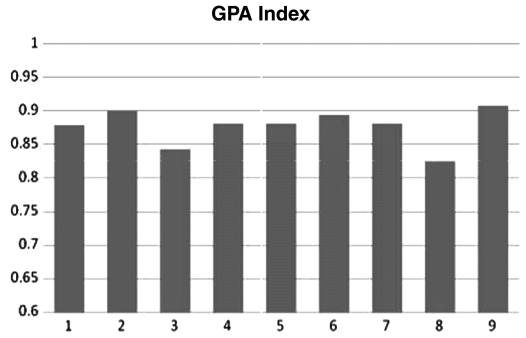

Fig. 17 GPA indices of case study 3.

solutions. On the contrary, the comparisons of predicted degradations with implanted degradations shown in Figs. 10–12, 14, and 15 indicate that the prediction accuracy is still satisfactory. Although the random measurement noise imposed on the fault signatures shown in Figs. 7, 8, and 16 does not represent the whole influence of measurement noise, the diagnostic results give an indication of how the measurement noise might affect the accuracy of the NLWLS diagnostic predictions.

The smearing effect (Fig. 11) due to the existence of measurement noise can be misleading and should be reduced if possible. By using the weighted result of the diagnostic predictions, the smearing effect of the prediction may be reduced to within 3% of degradation, which is equivalent to the impact of measurement noise.

The NLWLS approach is a model-based gas-turbine gas-path diagnostic method. Therefore, once the accurate nonlinear engine performance models are established, such a diagnostic approach can be applied to different gas-turbine engines. In addition, no heuristic maintenance and operational information is required by the NLWLS diagnostic approach.

Although it involves numerical iterations, the computation speed of the NLWLS approach is fast. For example, Fig. 18 shows the convergence process of compressor fault prediction with 55 iterations using the fault signature with measurement noise. It takes about 7 s for the calculation using a desktop computer with a 2.4 GHz dual processor. The computation speed of this diagnostic method (opposite to computation time) is relatively slower than that of linear GPA, neural network, and expert systems, comparable to the nonlinear GPA approach in [7,8], and much faster than model-based optimization approaches. The position of the NLWLS approach on the graph of computation speed and diagnostic algorithm complexity [22], compared with some other diagnostic methods, is shown in Fig. 19.

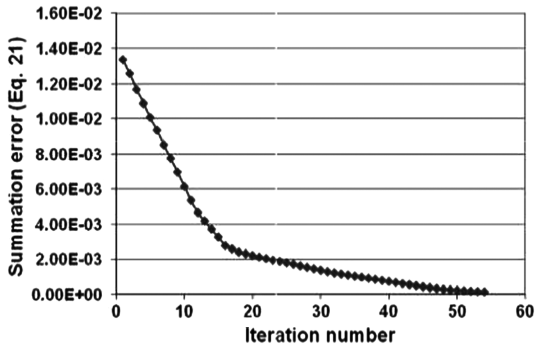

Fig. 18 Iteration process of NLWLS.

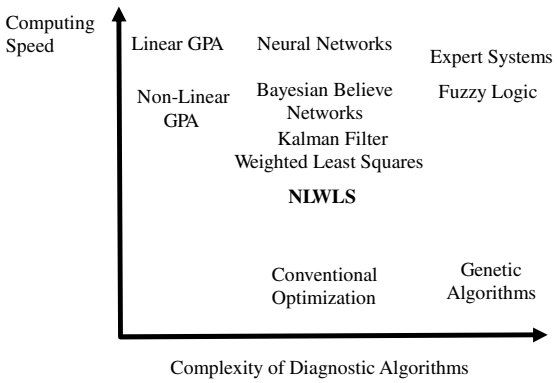

Fig. 19 Position of NLWLS approach on speed-complexity graph [22].

IV. Conclusions

A nonlinear weighted-least-squares (NLWLS) approach for gas-turbine gas-path diagnostics is introduced. The approach can be easily applied to different gas-turbine engines and provide satisfactory diagnostic predictions. Inclusion of random measurement noise imposed on individual samples in the analysis indicates that the approach is able to function well with measurement noise and offer results with accuracy acceptable for engineering applications. Enhanced with the concept of gas-turbine component fault cases and assessed with the GPA index, the NLWLS diagnostic approach is able to identify the most likely degraded engine components and satisfactorily quantify component degradations. When multiple fault cases are identified as the most likely fault cases, the weighted solution of the multiple fault cases can provide a solution with smaller smearing effects. The NLWLS approach has moderate model complexity compared with other gas-path diagnostic approaches and has similar computational speed to that of nonlinear GPA. The NLWLS approach has been applied to a model gas-turbine engine similar to the GE LM2500+ implanted with a single-component degradation and dual-component degradation. The diagnostic results in the three case studies provide promising results and illustrate the effectiveness and successful application of this diagnostic approach.

References

[1] Urban, L. A., "Gas Path Analysis Applied to Turbine Engine Condition Monitoring," AIAA Paper 72-1082, 1972.

[2] Doel, D. L., "An Assessment of Weighted-Least-Squares-Based Gas Path Analysis," *Journal of Engineering for Gas Turbines and Power*, Vol. 116, 1994, pp. 366–373. doi:10.1115/1.2906829

[3] Borguet, S., and Leonard, O., "A Generalized Likelihood Ratio Test for Adaptive Gas Turbine Performance Monitoring," *Journal of Engineering for Gas Turbines and Power*, Vol. 131, 2009, Paper 011601. doi:10.1115/1.2967493.

[4] Romessis, C., Kamboukos, Ph., and Mathioudakis, K., "The Use of Probabilistic Reasoning to Improve Least Squares Based Gas Path Diagnostics," *Journal of Engineering for Gas Turbines and Power*, Vol. 129, 2007, pp. 970–976. doi:10.1115/1.2436548

[5] Volponi, A. J., "Gas Path Analysis: An Approach to Engine Diagnostics," *35th Symposium Mechanical Failures Prevention Group*, Gaithersburg, MD, April 1982.

[6] Provost, M. J., "COMPASS: A Generalized Ground-Based Monitoring System," *Engine Condition Monitoring—Technology and Experience*, AGARD CP-449, Oct. 1988.

[7] Escher, P. C., and Singh, R., "An Object-Oriented Diagnostics Computer Program Suitable for Industrial Gas Turbines," *21st (CIMAC) International Congress of Combustion Engines*, 15–18 May 1995.

[8] Li, Y. G., and Singh, R., "An Advanced Gas Turbine Gas Path Diagnostic System—PYTHIA," XVII International Symposium on Air Breathing Engines, ISABE Paper 2005-1284, Munich, Sept. 2005.

[9] Li, Y. G., "Gas Turbine Performance and Health Status Estimation Using Adaptive Gas Path Analysis," ASME Turbo Expo, Paper GT2009-59168, 2009.

[10] Denney, G., "F16 Jet Engine Trending and Diagnostics with Neural Networks," *Proceedings of SPIE: The International Society for Optical Engineering*, Vol. 1965, 1993, pp. 419–422.

[11] Ogaji, S. O. T., and Singh, R., "Gas Path Fault Diagnosis Framework for a Three-Shaft Gas Turbine," *Proceedings of the Institution of Mechanical Engineers Part A, Journal of Power and Energy*, Vol. 217,

Part A, 2003, pp. 149–157.
doi:10.1243/09576500360611173
[12] Tan, H. S., "Fourier Neural Networks and Generalized Single Hidden Layer Networks in Aircraft Engine Fault Diagnostics," *Journal of Engineering for Gas Turbines and Power*, Vol. 128, 2006, pp. 773–782.
doi:10.1115/1.2179465
[13] Romessis, C., and Mathioudakis, K., "Bayesian Network Approach for Gas Path Fault Diagnosis," *Journal of Engineering for Gas Turbines and Power*, Vol. 128, 2006, pp. 64–72.
doi:10.1115/1.1924536
[14] Zedda, M., and Singh, R., "Gas Turbine Engine and Sensor Fault Diagnosis Using Optimization Techniques," *Journal of Propulsion and Power*, Vol. 18, No. 5, 2002, pp. 1019–1026.
doi:10.2514/2.6050
[15] Gulati, A., Zedda, M., and Singh, R., "Gas Turbine Engine and Sensor Multiple Operating Point Analysis Using Optimization Techniques," AIAA Paper 2000-3716, 2000.
[16] Wallin, M., and Grönstedt, T., "A Comparative Study of Genetic Algorithms and Gradient Methods for RM12 Turbofan Engine Diagnostics and Performance Estimation," ASME Turbo Expo Paper GT2004-53591, 2004.
[17] Ganguli, R., "Application of Fuzzy Logic for Fault Isolation of Jet Engines," ASME Turbo Expo Paper 2001-GT-0013, 2001.
[18] Martis, D., "Fuzzy Logic Estimation Applied to Newton Methods for Gas Turbines," *Journal of Engineering for Gas Turbines and Power*, Vol. 129, 2007, pp. 88–96.
doi:10.1115/1.2360597
[19] Eustace, R., "A Real-World Application of Fuzzy Logic and Influence Coefficients for Gas Turbine Performance Diagnostics," *Journal of Engineering for Gas Turbines and Power*, Vol. 130, 2008, Paper 061601.
doi:10.1115/1.2940989
[20] Li, Y. G., "A Gas Turbine Diagnostic Approach with Transient Measurement," *Proceedings of the Institution of Mechanical Engineers Part A, Journal of Power and Energy*, Vol. 217, Part A, 2003, pp. 169–172.
doi:10.1243/09576500360611317
[21] Surender, V. P., and Ganguli, R., "Adaptive Myriad Filter for Improved Gas Turbine Condition Monitoring Using Transient Data," *Journal of Engineering for Gas Turbines and Power*, Vol. 127, 2005, pp. 329–339.
doi:10.1115/1.1850491
[22] Li, Y. G., "Performance-Analysis-Based Gas Turbine Diagnostics: a Review," *Proceedings of the Institution of Mechanical Engineers Part A, Journal of Power and Energy*, Vol. 216, No. 5, 2002, pp. 363–377.
doi:10.1243/095765002320877856
[23] Singh, R., "Advances and Opportunities in Gas Path Diagnostics," *15th ISABE*, Paper 2003-1008, 2003.
[24] Jaw, L. C., "Recent Advances in Aircraft Engine Health Management (EHM) Technologies and Recommendations for the Next Step," ASME Turbo Expo Paper GT2005-68625, 2005.
[25] Chen, D.-G., and Zhu, Z.-L., "Model Identification-Based Fault Analysis Method Applied to Jet Engines," 14th ISABE, Paper 2001-1111, 2001.
[26] Korakianitis, T., and Wilson, D. G., "Models for Predicting the Performance of Brayton-Cycle Engines," *Journal of Engineering for Gas Turbines and Power*, Vol. 116, No. 2, April 1994, pp. 381–388.
doi:10.1115/1.2906831
[27] Korakianitis, T., and Beier, K., "Investigation of the Part-Load Performance of Two 1.12 MW Regenerative Marine Gas Turbines," *Journal of Engineering for Gas Turbines and Power*, Vol. 116, No. 2, April 1994, pp. 418–423.
doi:10.1115/1.2906837
[28] Korakianitis, T., and Svensson, K. "Off-Design Performance of Various Gas-Turbine Cycle and Shaft Configurations," *Journal of Engineering for Gas Turbines and Power*, Vol. 121, Oct. 1999, pp. 649–655.
doi:10.1115/1.2818521
[29] Korakianitis, T., Grantstrom, J., Wassingbo, P., and Massardo, A. F., "Parametric Performance of Combined-Cogeneration Power Plants with Various Power and Efficiency Enhancements," *Journal of Engineering for Gas Turbines and Power*, Vol. 127, No. 1, Jan 2005, pp. 65–72.
doi:10.1115/1.1808427
[30] Zwebek, A., and Pilidis, P., "Degradation Effects on Combined Cycle Power Plant Performance—Part I: Gas Turbine Cycle Component Degradation Effects," *Journal of Engineering for Gas Turbines and Power*, Vol. 125, No. 3, 2003, pp. 651–657.
doi:10.1115/1.1519271
[31] Pachidis, V., Pilidis, P., Marinai, L., Templalexis, I., "Towards a Full Two Dimensional Gas Turbine Performance Simulator," *The Aeronautical Journal*, Vol. 111, No. 1121, July 2007, pp. 433–442.
[32] Lambiris, B., Mathioudakis, K., Stamatis, A., and Papailiou, K., "Adaptive Modeling of Jet Engine Performance with Application to Condition Monitoring," *Journal of Propulsion and Power*, Vol. 10, No. 6, Nov.–Dec. 1994, pp. 890–896.
doi:10.2514/3.23828
[33] Mathioudakis, K., Kamboukos, Ph., and Stamatis, A., "Turbofan Performance Deterioration Tracking Using Non-Linear Models and Optimization Techniques," *Journal of Turbomachinery*, Vol. 124, 2002, pp. 580–587.
doi:10.1115/1.1512678
[34] Zedda, M., and Singh, R., "Gas Turbine Engine and Sensor Fault Diagnosis Using Optimisation Techniques," AIAA Paper 99-2530, 1999.
[35] Volponi, A. J., Depold, H., and Ganguli, R., "The Use of Kalman Filter and Neural Network Methodologies in Gas Turbine Performance Diagnostics: A Comparative Study," *Journal of Engineering for Gas Turbines and Power*, Vol. 125, No. 4, Oct. 2003, pp. 917–924.
doi:10.1115/1.1419016
[36] Macmillan, W. L., "Development of a Module Type Computer Program for the Calculation of Gas Turbine Off Design Performance," Ph.D. Thesis, Cranfield Univ., Cranfield, England, U.K., 1974.
[37] Dyson, R. J. E., and Doel, D. L., "CF-80 Condition Monitoring—The Engine Manufacturing's Involvement in Data Acquisition and Analysis," AIAA Paper 84-1412, 1987.

C. Tan
Associate Editor